Preparation and Characterization of Langmuir and Langmuir−Blodgett Films from a Nitrile-Terminated Tolan

Gorka Pera,[†] Ana Villares,[†] María Carmen López,[†] Pilar Cea,*[,†] Donocadh P. Lydon,[‡] and Paul J. Low[‡]

Departamento de Química Orgánica−Química Física, Área de Química Física, Facultad de Ciencias, Universidad de Zaragoza, 50009 Zaragoza, Spain, and Department of Chemistry, University of Durham, Durham DH1 3LE, United Kingdom

Received October 23, 2006. Revised Manuscript Received December 11, 2006

Langmuir and Langmuir−Blodgett films of a nitrile-terminated tolan, namely 4-[4′-decyloxyphenylethynyl]benzonitrile, have been fabricated and characterized at various surface pressures, with surface pressure and surface potential isotherms together with Brewster angle microscopy being used to map the different phases of the tolan monolayer at the air−water interface. The Langmuir films have been characterized by UV−vis spectroscopy, with quantitative analysis of the reflection spectra supporting an organizational model in which compression of the film leads to change in the tilt angle of the tolan molecules from an initial value of ca. 35° to one of ca. 60° before collapse of the monolayer. Moreover, a blue shift in the reflection spectrum of the Langmuir film of 30 nm with respect to the spectrum of a chloroform solution of the nitrile tolan indicates that two-dimensional H-aggregates are formed at the air−water interface. These structures represent a minimum free-energy conformation for the system, as they are observed even before the compression process starts. The monolayers are transferred undisturbed onto solid substrates, with atomic force microscopy revealing well-ordered films without three-dimensional defects.

Introduction

Molecular, oligomeric, and polymeric materials derived from the phenylene ethynylene motif are a source of great contemporary interest.[1−4] Various members of the phenylene ethynylene family have been shown to offer useful physical properties, including NLO response,[5,6] luminescence,[1,7,8] and electroluminescence.[9] The rigid molecular structure and ready functionalization of the aromatic fragments can be exploited in the design of liquid crystal mesogens.[10−15] The presence of an extended π-conjugated electronic structure along the long molecular axis has also resulted in an ever-growing number of oligomeric phenylene ethynylenes being investigated as molecular wires and other components for molecular electronics.[16−21]

Although liquid-crystalline systems might be considered to be self-organizing, with the liquid crystalline behavior being a direct consequence of the physical structure of the molecular framework, in general, fabrication of devices based on molecular materials demands consideration of how best to achieve a desired arrangement, distribution, and/or alignment of the molecules of interest within the device structure. Solution casting methods are appealing for industrial large transfer processing; however, they present the disadvantage of preventing strict thickness and precise control over the molecular architecture and arrangement. Self-assembly (SA) techniques have been demonstrated to produce molecular monolayers of functionalized molecules on a wide range of surfaces, with the assembly of thiols on gold being particularly common and giving rise to excellent quality films formed by the strong gold−sulfur linkage.[22−26] However,

* To whom correspondence should be addressed. E-mail: pilarcea@unizar.es.
[†] Universidad de Zaragoza.
[‡] University of Durham.

(1) Bunz, U. H. F. *Chem. Rev.* **2000**, *100*, 1605.
(2) Bunz, U. H. F. *Acc. Chem. Res.* **2001**, *34*, 988.
(3) Bunz, U. H. F. *Adv. Polym. Sci.* **2005**, *177*, 1.
(4) Martin, R. E.; Diederich, F. *Angew. Chem., Int. Ed.* **1999**, *38*, 1350.
(5) Wong, M. S.; Nicoud, J. F. *Tetrahedron Lett.* **1994**, *35*, 6113.
(6) Polin, J.; Buchmeiser, M.; Nock, H.; Schottenberger, H. *Mol. Cryst. Liq. Cryst. Sci. Technol., Sect. A* **1997**, *293*, 287.
(7) Beeby, A.; Findlay, K.; Low, P. J.; Marder, T. B. *J. Am. Chem. Soc.* **2002**, *124*, 8280.
(8) Franke, V.; Mangel, T.; Müllen, K. *Macromolecules* **1998**, *31*, 2447.
(9) Breen, C. A.; Tischler, J. R.; Bulovic, V.; Swager, T. M. *Adv. Mater.* **2005**, *17*, 1981.
(10) Lydon, D. P.; Porres, L.; Beeby, A.; Marder, T. B.; Low, P. J. *New J. Chem.* **2005**, *15*, 4854.
(11) Carbonnier, B.; Egbe, D. A. M.; Birckner, E.; Grummt, U. W.; Pakula, T. *Macromolecules* **2005**, *38*, 7546.
(12) Lehmann, M.; Levin, J. M. *Mol. Cryst. Liq. Cryst.* **2004**, *411*, 1315.
(13) Brunsveld, L.; Folmer, B. J. B.; Meijer, E. W.; Sijbesma, R. P. *Chem. Rev.* **2001**, *101*, 4071.
(14) Huang, W. Y.; Gao, W.; Kwei, T. K.; Okamoto, Y. *Macromolecules* **2001**, *34*, 1570.
(15) Mio, M. J.; Prince, R. B.; Moore, J. S.; Kuebel, C.; Martin, D. C. *J. Am. Chem. Soc* **2000**, *122*, 6134.
(16) James, D. K.; Tour, J. M. *Top. Curr. Chem.* **2005**, *257*, 33.
(17) James, D. K.; Tour, J. M. *Chem. Mater.* **2004**, *16*, 4423.
(18) Yin, X.; Liu, H. M.; Zhao, J. W. *J. Chem. Phys.* **2006**, *125*, 094711.
(19) Hu, W. P.; Nakashima, H.; Furukawa, K.; Kashimura, Y.; Ajito, K.; Liu, Y. Q.; Zhu, D. B.; Torimitsu, K. *J. Am. Chem. Soc.* **2005**, *127*, 2804.
(20) Fan, F. R. F.; Yang, J. P.; Cai, L. T.; Price, D. W.; Dirk, S. M.; Kosynkin, D. V.; Yao, Y. X.; Rawlett, A. M.; Tour, J. M.; Bard, A. J. *J. Am. Chem. Soc.* **2002**, *124*, 5550.
(21) Bumm, L. A.; Arnold, J. J.; Cygan, M. T.; Dunbar, T. D.; Burgin, T. P.; Jones, L., II; Allara, D. L.; Tour, J. M.; Weiss, P. S. *Science* **1996**, *271*, 1705.
(22) Nuzzo, R. G.; Allara, D. L. *J. Am. Chem. Soc.* **1983**, *105*, 4481.

10.1021/cm062524p CCC: $37.00
Published on Web 01/23/2007

certain drawbacks to the thiol-on-gold SA technique have been described, including the tendency of organic thiols to oxidize to disulfides.[27] Although the use of protected thiols can alleviate this problem, the incorporation of extraneous material within the system when in situ deprotection steps are employed has also been described,[28] which can add a degree of additional complexity to the process. To further complicate studies based on gold−thiol self-assembled monolayers (SAM), the gold−sulfur bond is rather fluxional, and changes in the gold−sulfur interaction are now thought to be largely responsible for the dynamic switching of conductivity observed in early studies of single-molecule conductivity.[29−31]

The Langmuir−Blodgett (LB) method is also an excellent tool with which to fabricate films with a high internal order.[32−37] The LB technique provides control over the desired number of layers deposited on a surface and is therefore well-suited to the production of both mono- and multilayer structured films. In addition, by making use of the wide variety of polar functional groups that can be physically or chemically adsorbed onto different substrates, it is possible to use LB methods to fabricate structures featuring any one of a large number of organic−metal interfaces. This is especially important given the crucial role the metal−molecule interface plays in, for example, measurements of the conductivity of single molecules.[26,38−44] The use of oriented molecular films prepared using LB methods could therefore provide a simple base from which to explore a very wide variety of organic−metal contacts (e.g., nitrile, amine, carboxylic acid, etc., on Pt, Pd, Ag, etc.).[45−48]

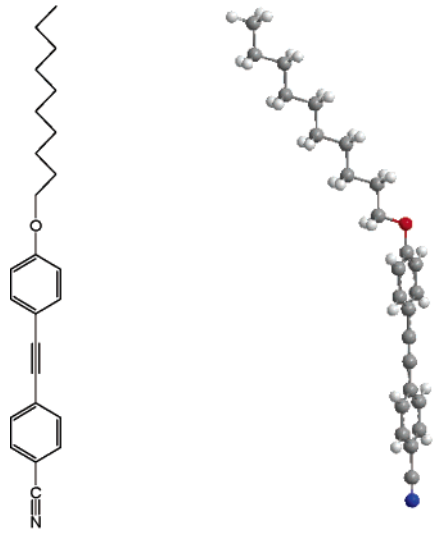

Figure 1. Chemical structure (left) and space-filling molecular model (right) of 4-[4′-decyloxyphenylethynyl]benzonitrile (C10(PEB)CN).

In contrast to the large body of published work describing fabrication and properties of oligomeric phenylene ethynylene derivatives in gold−thiol-based SAM, there is comparatively little data available in the literature for the detailed process of fabrication of LB films of oligomeric phenylene ethynylenes (OPE)-based compounds and the precise organization of the molecules within these films. This has motivated us to pursue the preparation of a series of phenylene-ethynylene-based compounds suitable for the fabrication of well-ordered Langmuir and Langmuir−Blodgett films. The ultimate goal of this study is a comprehensive analysis of the influence different functional polar groups and molecular geometries within the OPE structure on the intermolecular interactions, aggregation effects, and local molecular environment within the film, as well as the orientation of the molecules in the film. All of these factors will play a role in moderating the electronic and optical properties of the films.

This paper reports the synthesis of 4-[4′-decyloxyphenylethynyl]benzonitrile (Figure 1), henceforward abbreviated as C10(PEB)CN, the Langmuir and LB film forming behavior of this compound, and characterization of the resulting films. The compound C10(PEB)CN features a polar nitrile end group, which facilitates the spreading of the molecule as well as its anchoring onto the water surface. Moreover, the hydrophobic phenylene ethynylene core and a relatively long alkyl chain prevent C10(PEB)CN from being dissolved in water and provide stability to the monolayer thanks to lateral $\pi-\pi$ and van der Waals interactions with neighboring

(23) Dhirani, A.; Zehner, R. W.; Hsung, R. P.; Guyot-Sionnest, P.; Sita, L. R. *J. Am. Chem. Soc.* **1996**, *118*, 3319.
(24) Lin, P. H.; Guyot-Sionnest, P. *Langmuir* **1999**, *15*, 6825.
(25) Ciszek, J. W.; Stewart, M. P.; Tour, J. M. *J. Am. Chem. Soc.* **2004**, *126*, 13172.
(26) Lewis, P. A.; Inman, C. E.; Maya, F.; Tour, J. M.; Hutchison, J. E.; Weiss, P. S. *J. Am. Chem. Soc.* **2005**, *127*, 17421.
(27) Tour, J. M.; Jones, L., II; Pearson, D. L.; Lamba, J. J. S.; Burgin, T. P.; Whitesides, G. M.; Allara, D. L.; Parikh, A. N.; Atre, S. V. *J. Am. Chem. Soc.* **1995**, *117*, 9529.
(28) Stapleton, J. J.; Harder, P.; Daniel, T. A.; Reinard, M. D.; Yao, Y.; Price, D. W.; Tour, J. M.; Allara, D. L. *Langmuir* **2003**, *19*, 8245.
(29) Ramachandran, G. K.; Hopson, T. J.; Rawlett, A. M.; Nagahara, L. A.; Primak, A.; Lindsay, S. M. *Science* **2003**, *300*, 1413.
(30) Keane, Z. K.; Ciszek, J. W.; Tour, J. M.; Natelson, D. *Nano Lett.* **2006**, *6*, 1518.
(31) Yasuda, S.; Yoshida, S.; Sasaki, J.; Okutsu, Y.; Nakamura, T.; Taninaka, A.; Takeuchi, O.; Shigekawa, H. *J. Am. Chem. Soc* **2006**, *128*, 7746.
(32) Roberts, G. *Langmuir−Blodgett Films*; Plenum Press: New York, 1990.
(33) Ulman, A. *An Introduction to Ultrathin Organic Films: From Langmuir−Blodgett to Self-Assembly*; Academic Press: San Diego, 1991.
(34) Peterson, I. R.; Mahler, G.; May, V.; Schreiber, M. *The Molecular Electronic Handbook*; Marcel Dekker: New York, 1994.
(35) Tredgold, R. H. *Order in Thin Organic Films*; Cambridge University Press, 1994.
(36) Bryce, M. R.; Petty, M. C. *Nature* **1995**, *334*, 771.
(37) Petty, M. C.; Bryce, M. R.; Bloor, D. *Introduction to Molecular Electronics*; Oxford University Press: New York, 1995.
(38) Zhu, X. Y.; Vondrak, T.; Wang, H.; Gahl, C.; Ishioka, K.; Wolf, M. *Surf. Sci.* **2000**, *451*, 244.
(39) Beebee, J. M.; Engeelkes, V. B.; Miller, L. L.; Frisbie, C. D. *J. Am. Chem. Soc.* **2002**, *124*, 11268.
(40) Fan, F.-R. F.; Yao, Y.; Cai, L.; Cheng, L.; Tour, J. M.; Bard, A. J. *J. Am. Chem. Soc.* **2004**, *126*, 4035.
(41) Cai, L.; Cabassi, M. A.; Yoon, H. C.; Cabarcos, O. M.; McGuiness, C. L.; Flatt, A. K.; Allara, D. L.; Tour, J. M.; Mayer, T. S. *Nano Lett.* **2005**, *5*, 2365.
(42) Xue, Y. Q.; Datta, S.; Ratner, M. A. *J. Chem. Phys.* **2001**, *115*, 4292.
(43) Kushmerick, J. G.; Holt, D. B.; Yang, J. C.; Naciri, J.; Moore, M. H.; Shashidhar, R. *Phys. Rev. Lett.* **2002**, *89*, 086802.
(44) Pérez-Jiménez, A. J. *J. Phys. Chem. B* **2005**, *109*, 10052.
(45) Stapleton, J. J.; Daniel, T. A.; Uppili, S.; Carbarcos, O. M.; Naciri, J.; Shashidhar, R.; Allara, D. L. *Langmuir* **2005**, *21*, 11061.
(46) Chabinyc, M. L.; Holmlin, R. W.; Haag, R.; Chen, X. X.; Ismagilov, R. F.; Rampi, M. A.; Whitesides, G. M. *ACS Symp. Ser.* **2003**, *844*, 16.
(47) Love, J. C.; Wolfe, B. D.; Haasch, R.; Chabinyc, M. L.; Paul, K. E.; Whitesides, G. M.; Nuzzo, R. G. *J. Am. Chem. Soc.* **2003**, *125*, 2597.
(48) Rampi, M. A.; Whitesides, G. M. *Chem. Phys.* **2002**, *281*, 373.

molecules. The detailed organization of C10(PEB)CN molecules within Langmuir monolayers and the final architecture of the LB films have been thoroughly studied by optical, spectroscopic, and microscopic procedures.

Experimental Section

Synthesis. All reactions were carried out under an atmosphere of nitrogen using standard Schlenk techniques. Reaction solvents were distilled from CaH_2 and degassed before use. No special precautions were taken to exclude air or moisture during workup. The compounds 4-decyloxyiodobenzene,[49,50] $PdCl_2(PPh_3)_2$,[51] and 4-ethynyl-1-decyloxybenzene[52] were prepared by the literature methods, or minor variation as described below. Other reagents were purchased and used as received.

NMR spectra were recorded on a Bruker Avance (^{1}H 400.13 MHz, ^{13}C 100.61 MHz, ^{31}P 161.98 MHz) or Varian Mercury (^{31}P 161.91 MHz) spectrometer from $CDCl_3$ solutions and referenced against solvent resonances (^{1}H, ^{13}C) or external H_3PO_4 (^{31}P). IR spectra were recorded using a Nicolet Avatar spectrometer from solutions in a cell fitted with CaF_2 windows.

Preparation of 4-Ethynyl-decyloxybenzene. A Schlenk flask was charged with HC≡CSiMe$_3$ (2.66 g, 2.71 × 10^{-2} mol), 4-decyloxyiodobenzene (8.90 g, 2.47 × 10^{-2} mol), CuI (0.047 g, 2.47 × 10^{-4} mol), $PdCl_2(PPh_3)_2$ (0.173 g, 2.47 × 10^{-4} mol), and NEt_3 (50 mL), and the reaction mixture was allowed to stir overnight. The ammonium salt byproduct that had precipitated was removed by filtration and washed with toluene. The washings were combined with the filtrate and the solvent evaporated under reduced pressure to yield the crude product, which was purified by flash chromatography on silica gel (hexane). The purified 4-(trimethylsilylethynyl)decyloxybenzene was stirred with a suspension of potassium carbonate in 1:1 methanol:THF (6 h) before the solvent was removed in vacuo. The residue was extracted with diethyl ether, and the extracts were washed with water (2 × 50 mL). A further cycle of solvent removal, extraction (CH_2Cl_2), and water washing afforded the terminal alkyne, which was sufficiently pure to be used directly in subsequent reactions. Yield: 5.27 g, 2.04 × 10^{-2} mol, 83%. ^{1}H NMR: δ 7.43 (AA′XX′, 2H, Ar*H*); 6.83 (AA′XX′, 2H, Ar*H*); 3.95 (t, ^3J(H,H) = 6.4 Hz, 2H, OC*H*$_2$R); 3.00, (s, 1H, C≡C*H*); 1.77 (m, 2H, C*H*$_2$-aliphatic); 1.33 (m, 14H, C*H*$_2$-aliphatic); 0.91 (t ^3J(HH) = 6.8 Hz 3H, C*H*$_3$). ^{13}C NMR: δ 159.7, 134.1, 114.7, 114.0, (Ar); 84.1, 75.9, (*C*≡*C*); 68.2, (O*C*H$_2$−R); 32.0, 29.7, 29.7×, 29.5, 29.45, 29.3, 26.1, 22.8, (aliphatic); 14.2, (*C*H$_3$). IR (KBr plates, neat): ν(C≡C−H) 3316, 3291; ν(C≡C) 2107 cm^{-1}.

Preparation of 4-Decyloxyphenylethynylbenzonitrile. 4-Ethynyl-decyloxybenzene (1.50 g, 5.81 × 10^{-3} mol) was added to a Schlenk flask containing 4-bromobenzonitrile (1.06 g, 5.81 × 10^{-5} mol), CuI (0.011 g, 5.81 × 10^{-5} mol), and $PdCl_2(PPh_3)_2$ (0.041 g, 5.81 × 10^{-5} mol) in triethylamine (50 mL). The reaction mixture was heated at reflux (16 h) and then allowed to cool. The crude reaction mixture was filtered to remove the precipitated ammonium salt, and the filtrate was evaporated to dryness under reduced pressure. The crude product was purified by column chromatography on silica gel using 1:2 CH_2Cl_2:hexane as eluant. The yellow solid obtained was then recrystallized in toluene:hexane to give the pure product. Yield: 0.80 g, 2.23 × 10^{-3} mol, 40%. ^{1}H NMR: δ 7.55 (AA′XX′, 2H, Ar*H*); 7.50 (AA′XX′, 2H, Ar*H*); 7.39 (AA′XX′, 2H, Ar*H*); 6.81 (AA′XX′, 2H, Ar*H*); 3.97 (t, ^3J(H,H) = 6.4 Hz, 2H, OC*H*$_2$R); 1.80 (m 2H, CH$_2$-aliphatic); 1.45 (m, 14H, CH$_2$-aliphatic); 0.89 (t ^3J(HH) = 7.2 Hz 3H, C*H*$_3$). ^{13}C NMR: δ 159.4, 133.3, 132.0, 131.8, 128.6, 118.6, 114.7, 113.9, 111.0, (Ar); 94.3, 86.7, (*C*≡*C*); 68.2, (O*C*H$_2$−R); 31.9, 29.56, 29.7, 29.4, 29.3, 29.2, 26.0, 22.7, (aliphatic); 14.1, (*C*H$_3$). $C_{25}H_{29}NO$ EI-MS: 358.9 (46) [M]$^+$, 218.7, (100) [M−$C_{10}H_{21}$]$^+$. Requires: C, 83.52; H, 8.13; N, 4.45. Found: C, 83.66; H, 8.21; N, 4.08.

Film Fabrication. The films were prepared on a Nima Teflon trough with dimensions of 720 × 100 mm^2 that was housed in a constant-temperature (20 ± 1 °C) clean room. The surface pressure (π) of the monolayers was measured by a Wilhelmy paper plate pressure sensor. The subphase was water (Millipore Milli-Q, resistivity 18.2 MΩ·cm). A solution of 4-[4′-decyloxyphenylethynyl]-benzonitrile in chloroform (HPLC grade, 99.9%, purchased from Aldrich and used as received) was delivered from a syringe held very close to the surface, allowing the surface pressure to return to a value as close as possible to zero between each addition. The solvent was allowed to completely evaporate over a period of at least 15 min before compression of the monolayer commenced at a constant sweeping speed of 0.50 nm^2 molecule^{-1} min^{-1}. Each compression isotherm was registered at least three times to ensure the reproducibility of results. The $\Delta V-A$ measurements were carried out using a Kelvin Probe provided by Nanofilm Technologie GmbH, Göttingen, Germany. A commercial mini-Brewster angle microscope (mini-BAM), also from Nanofilm Technologie, was employed for the direct visualization of the monolayers at the air−water interface, and a commercial UV−vis reflection spectrophotometer, detailed described in a recent paper,[53] was used to obtain the reflection spectra of the Langmuir films during the compression process.

The solid substrates used for the transferences (quartz and mica for the UV−vis and AFM measurements, respectively) were cleaned carefully, as described elsewhere.[54,55] The monolayers were deposited at a constant surface pressure by the vertical dipping method, and the dipping speed was 6 mm/min. Quartz crystal microbalance (QCM) measurements were carried out using a Stanford Research System instrument and employing AT-cut, α-quartz crystals with a resonance frequency of 5 MHz having circular gold electrodes patterned on both sides. UV−vis spectra of the LB films were acquired on a Varian Cary 50 spectrophotometer and recorded using a normal incident angle with respect to the film plane. The atomic force microscopy (AFM) experiments were performed by means of a multimode extended microscope with Nanoscope IIIA electronics from Digital Instruments operating at ambient atmosphere. All the images were recorded at room-temperature using the tapping mode.

Results and Discussion

Langmuir Films. The compound C10(PEB)CN has a rigid molecular structure with a conjugated π-electron system. In a manner entirely analogous to other amphiphilic molecules containing large polyaromatic moieties,[56] C10(PEB)CN has a large tendency to aggregate due to strong $\pi-\pi$ interactions. Thus, the Beer−Lambert law is only followed at relatively low concentrations (<1 × 10^{-4} M). Consequently, very dilute

(49) Bruce, D. W.; Dunmur, D. A.; Lalinde, E.; Maitlis, P. M.; Styring, P. *Liq. Cryst.* **1988**, *3*, 385.
(50) Mayershofer, M. G.; Wagner, M.; Udo, A.; Nuyken, O. *J. Polym. Sci., Part A: Polym. Chem.* **2004**, *42*, 4466.
(51) Clark, H. C.; Dixon, K. R. *J. Am. Chem. Soc.* **1969**, *91*, 596.
(52) Lee, S. J.; Park, C. R.; Chang, J. Y. *Langmuir* **2004**, *20*, 9513.
(53) Cea, P.; Martín, S.; Villares, A.; Möbius, D.; López, M. C. *J. Phys. Chem. B* **2006**, *110*, 963.
(54) Cea, P.; Lafuente, C.; Urieta, J. S.; López, M. C.; Royo, F. M. *Langmuir* **1997**, *13*, 4892.
(55) Haro, M.; Giner, B.; Lafuente, C.; López, M. C.; Royo, F. M.; Cea, P. *Langmuir* **2005**, *21*, 2796.
(56) Kaji, H.; Shimoyama, Y. *Jpn. J. Appl. Phys.* **2001**, *40*, 1396.

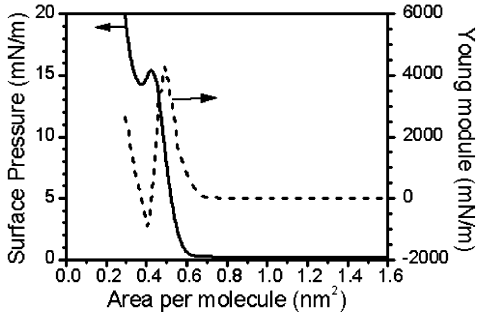

Figure 2. $\pi-A$ (left) isotherm and Young module vs area per molecule (right) for C10(PEB)CN.

solutions are required to fabricate true monolayers at the air−water interface.

A preliminary investigation of the formation of Langmuir films of C10(PEB)CN involving both the concentration and the volume of the spreading solution was carried out, and we concluded that only solutions of 1×10^{-5} M or lower concentration yield reproducible isotherms, provided the spreading volume is low enough (5 mL or lower for our trough dimensions). Under these conditions, a reproducible isotherm is routinely obtained (Figure 2). The take off in the isotherm takes place at ca. 0.65 nm^2/molecule. The surface pressure increases monotonously upon compression until an overshoot is reached. The presence of overshoots in $\pi-A$ isotherms is well-known and can be variously attributed to (i) slow rearrangement of the headgroups,[57] (ii) a lack of nucleation for the growth domains during the nonequilibrium compression process,[58] (iii) formation of well-ordered multilayer structures,[59] or (iv) collapse of the monolayer into undefined multilayer structures.[60] The collapse of Langmuir films comprised of nitrile amphiphiles at relatively low surface pressures have been reported and attributed to the relatively low polar character of this group that does not produce an effective anchoring of the amphiphile to the water surface.[61,62] The presence of plateaus (regions of constant surface pressure with decreasing area) in surface pressure isotherms is commonly observed when an ordered collapse leading to bilayer or trilayer formations occurs.[59] The absence of plateaus in the $\pi-A$ isotherm of C10(PEB)CN, together with other observations that will be discussed later, is indicative of a collapse of the C10(PEB)CN monolayer into an undefined multilayer structure.

Figure 2 also shows the Young module, K_s, defined as the inverse of the monolayer compressibility, given by[63]

$$K_s = -A\left(\frac{\partial \pi}{\partial A}\right)_T \qquad (1)$$

The Young module has been used as an indication of the phase state of the monolayer, with values higher than 1000 mN/m indicative of a solid phase.[64] The large values of the Young module achieved for C10(PEB)CN are also indicative of strong intermolecular interactions within the Langmuir film as well as the formation of a relatively rigid monolayer.[64]

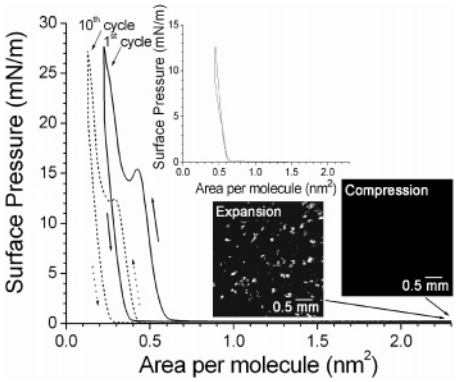

Figure 3. Hysteresis cycles and BAM images recorded before the first compression and after the first compression−expansion cycle.

To provide insight into the origin of the overshoot, the behavior of the $\pi-A$ isotherm during repeated cycles of compression and expansion was examined. If the barrier direction is reversed before the overshoot is reached, the hysteresis in the isotherm is negligible (inset Figure 3); however, the hysteresis in the isotherm is quite significant when the overshoot is passed on the compression cycle. Figure 3 shows the first and tenth compression and expansion isotherms of a series of consecutive cycles. When successive cycles are recorded, there is a decrease in the area per molecule, suggesting a loss of molecules from the monolayer. Figure 3 also shows the BAM images taken just after the spreading process and at the same area per molecule after the first compression−expansion cycle. Before the first compression, no domains or microcrystals are detectable within the instrument resolution, in the micrometer range. However, at the same area per molecule, BAM images taken after the first hysteresis cycle in which the overshoot is overcome shows the presence of microcrystals, suggesting an irreversible expelling of the molecules from the monolayer that leads to 3D structures.

BAM images recorded during the compression process are shown in Figure 4. At a surface pressure of 11 mN/m, the monolayer covers practically the whole water surface. At higher surface pressures, the BAM images show a similar aspect but are even more brilliant, suggesting a progressive tilt of the molecules to a more vertical position, i.e., a thicker monolayer.

The $\Delta V-A$ isotherm is illustrated in Figure 5, together with the $\pi-A$ isotherm for comparison purposes. The $\Delta V-A$ isotherm can often provide useful information relating to the molecular order within the monolayer, showing phase changes a few square Ångstroms before they are detected in the $\pi-A$ isotherm; this can be clearly seen in the case of the C10(PEB)CN (Figure 5). Compression of the C10(PEB)-CN monolayer results in an increase of the surface potential followed by a wide plateau ranging from 0.47 to 0.38 nm^2, after which a drastic drop in ΔV values occurs. The increase

(57) Mertesdorf, C.; Ringsdorf, H. *Liq. Cryst.* **1989**, *5*, 1757.
(58) Hui, S. W.; Yu, H. *Langmuir* **1992**, *8*, 2724.
(59) Cea, P.; Lafuente, C.; Urieta, J. S.; López, M. C.; Royo, F. M. *Langmuir* **1996**, *12*, 5881.
(60) McFate, C.; Ward, D.; Olmsted, J. I. *Langmuir* **1993**, *9*, 1036.
(61) Endrle, T.; Meixer, A. J.; Zschokke-Gränacher, I. *J. Chem. Phys.* **1994**, *101*, 4365.
(62) Martynski, T.; Hertmanowski, R.; Bauman, D. *Liq. Cryst.* **2001**, *28*, 437.
(63) Adamson, A. W.; Gast, A. P. *Physical Chemistry of Surfaces*, 6th ed.; John Wiley & Sons: New York, 1997.
(64) Davies, J. T.; Rideal, E. K. *Interfacial Phenomena;* Academic Press: New York, 1963.

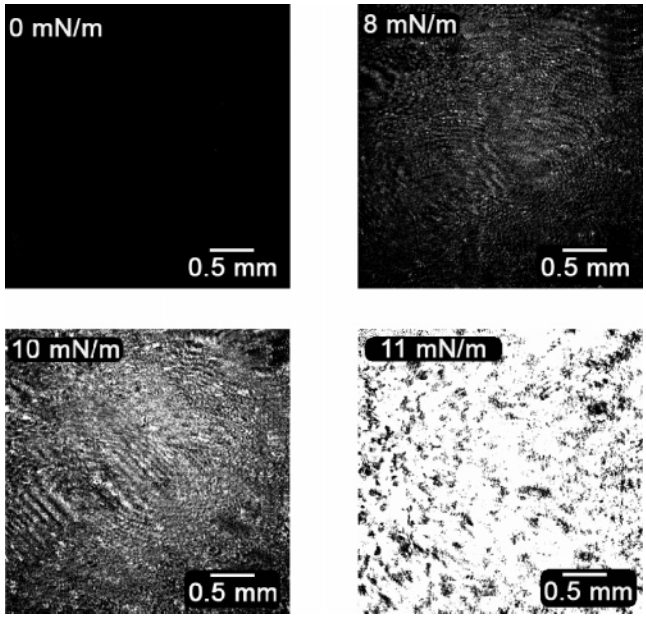

Figure 4. BAM images recorded upon the compression process at the indicated surface pressures.

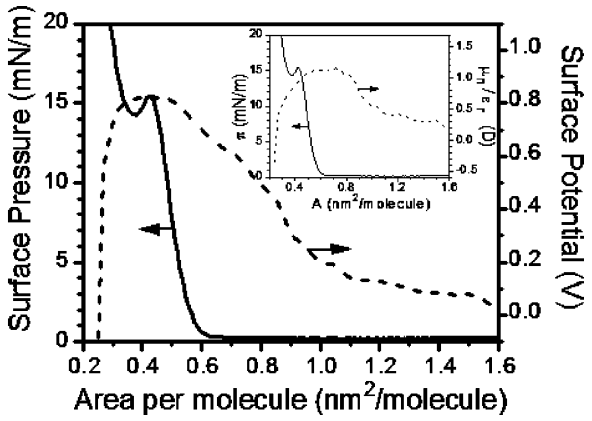

Figure 5. $\pi-A$ (left) and $\Delta V-A$ (right) isotherms for C10(PEB)CN. Inset graph shows the $\pi-A$ isotherm (left) and μ_n/ϵ_r values upon compression (right).

in ΔV with decreasing area per molecule is observed at higher values of the area per molecule than those corresponding to the increase in the surface pressure in the π-A isotherm. This is indicative of a progressive orientation of the molecules even in the gas phase where $\pi \rightarrow 0$. We will see later that other experimental data (reflection spectroscopy, Figures 6 and 7) also lead to this conclusion. For monolayers of amphiphilic compounds, a quantitative relationship between measured ΔV and the normal component of the dipole moment has been established by means of models based on the Helmholtz equation.[65] Thus, for a non-ionized monolayer, the surface potential can be expressed as

$$\Delta V = \frac{\mu_n}{A\epsilon_r\epsilon_0} \qquad (2)$$

where A is the area per molecule, ϵ_r and ϵ_0 are the relative dielectric constant and the permittivity of vacuum, respectively, and μ_n is the normal component of the dipole moment per molecule. The inset of Figure 5 shows μ_n/ϵ_r vs area per molecule with initially positive values for μ_n/ϵ_r that increase upon compression, which is indicative of dipole moment vectors directed from the water toward the air.[66] Before the drop at 0.47 nm^2, μ_n/ϵ_r values are around 1.1 D, which can be considered as a polarity measurement of the fully packed film. This value represents an additive contribution from the C10(PEB)CN dipole moment and the presence of ordered water molecules at the air−water interface.[67] On the other hand, the experimental $\Delta V-A$ data are consistent with the overshoot being caused by collapse of the monolayer with dipole moments randomly distributed in a three-dimensional arrangement of C10(PEB)CN molecules, which leads to a sudden decrease in ΔV as well as μ_n/ϵ_r and even negative values at low areas per molecule. It is noted at this point that transitions to a more condensed phase are characterized by an increase in ΔV values.

Reflection spectroscopy is a useful method for the in situ characterization of the monolayer at the air−water interface. In addition, molecular orientation and aggregation can be investigated more directly by spectroscopic methods than is achievable using the classic monolayer techniques described above.[53,68,69] Thus, in this work, we have determined the molecular orientation of the tolan derivative upon the compression process from reflection spectra, measured using unpolarized light under normal incidence. The reflection spectra recorded at different values of the area per molecule upon the compression process are illustrated in Figure 6a, together with the absorption spectrum of a dilute C10(PEB)-CN solution in chloroform and the normalized spectra in Figure 6b. The normalized reflection, ΔR_n, defined as $\Delta R_n = \Delta R \cdot$Area per molecule, more clearly demonstrates changes of orientation and/or association than the directly measured spectra, ΔR. The first remarkable characteristic is the blue shift in the reflection spectra by ca. 30 nm relative to the solution spectrum, consistent with the formation of H-aggregates. H-aggregates are often found in LB films formed from, for example, amphiphilic *trans*-stilbenes,[56,70] *trans*-azobenzenes,[69,71] hemicyanine derivatives,[72] squaraines,[73] and many other molecules in which the chromophore has the main dipole transition moment arranged more or less along the amphiphile backbone. It is also noteworthy that the hypsochromic shift of the floating layer is persistent and practically independent of the applied surface pressure. These observations indicate that the arrangement observed in the Langmuir film must represent a minimum free-energy conformation for the system and suggests that the formation of the blue-shifted aggregate does not depend for its formation upon the orientation imposed by the Langmuir technique.

(65) Helmholtz, H. *Abh. Thermodyn.* **1902**, *51*.
(66) Vogel, V.; Möbius, D. *J. Colloid Interface Sci.* **1988**, *126*, 408.
(67) Tsukanova, V.; Salesse, C. *J. Phys. Chem. B* **2004**, *108*, 10754.
(68) Orrit, M.; Möbius, D.; Lehman, U.; Meyer, H. *J. Chem. Phys.* **1986**, *85*, 4966.
(69) Pedrosa, J. M.; Martín-Romero, M. T.; Camacho, L. *J. Phys. Chem. B* **2002**, *106*, 2583.
(70) Furman, I.; Geiger, H. C.; Whitten, D. G.; Penner, T. L.; Ulman, A. *Langmuir* **1994**, *10*, 837.
(71) Song, X.; Perlstein, J.; Whitten, D. G. *J. Am. Chem. Soc.* **1995**, *117*, 7816.
(72) Heeseman, J. *J. Am. Chem. Soc.* **1980**, *102*, 2166.
(73) Chen, H.; Law, K.-Y.; Whitten, D. G. *J. Phys. Chem.* **1996**, *100*, 5949.

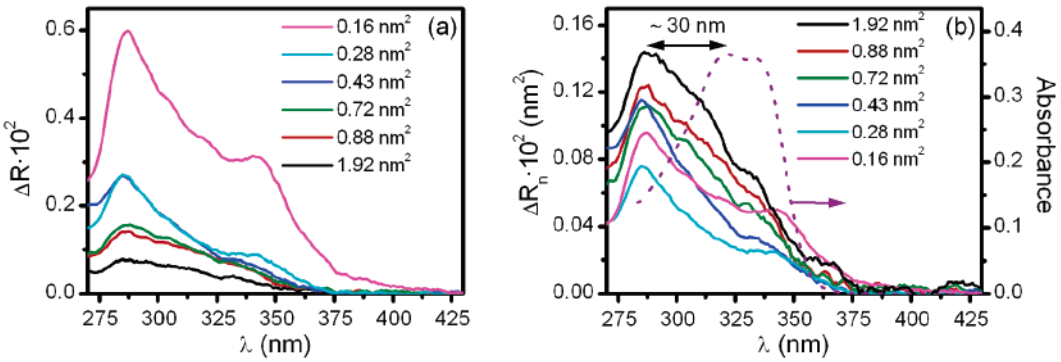

Figure 6. (a) Reflection spectra of Langmuir films upon compression. (b) Normalized reflection spectra upon compression and (dotted line) absorption spectra of a 8×10^{-6} M C10(PEB)CN solution in chloroform.

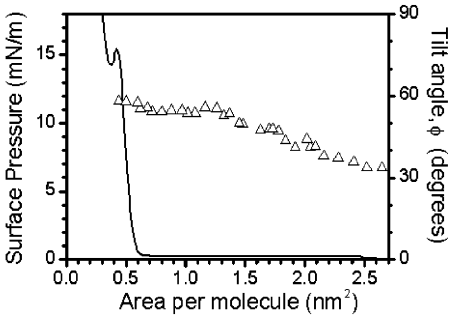

Figure 7. $\pi-A$ isotherm (left) and tilt angle of C10(PEB)CN upon the compression process (right).

Scheme 1. Definition of θ Angle (angle between the normal to the surface and the transition moment of the C10(PEB)CN molecule) and Its Complementary Angle ϕ

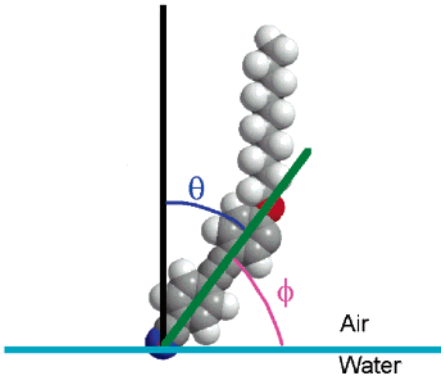

A quantitative analysis of the reflection spectra of C10(PEB)CN and a comparison of the reflection spectra with the UV−vis spectrum obtained in dilute solution has allowed us to calculate the tilt angle of the molecule with respect to the water surface. Thus, in solution, the orientation of the chromophore units is random and, therefore, the absorption must be proportional to a factor of 2/3 given that only two out of the three components of the transition moment of the chromophore are interacting with the incident unpolarized light.[69] Nevertheless, at the air−water interface, there is a preferential orientation of the chromophore that changes under compression; therefore, an orientation factor can be defined.[69] For a general case, assuming a homogeneous distribution of the C10(PEB)CN transition

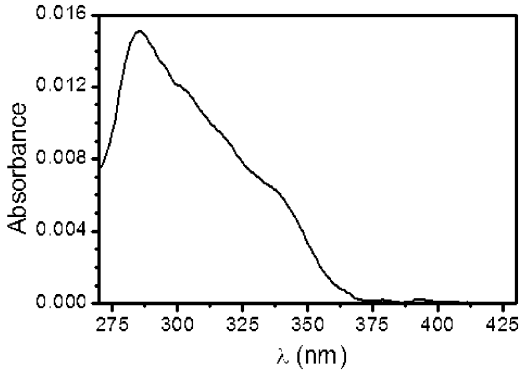

Figure 8. UV−vis spectrum of a monolayer LB film of C10(PEB)CN transferred at 10 mN/m.

moment around the surface normal, the orientation factor is defined by[69]

$$f_{\text{orient}} = \frac{3}{2}\sin^2\theta \tag{3}$$

where θ is the angle formed by the normal to the surface and the dipole transition moment of the chromofore (Scheme 1). The decrease in ΔR_n with increasing surface pressure (or decreasing area per molecule) observed in Figure 6b is related to an increase in the tilt angle of the C10(PEB)CN molecule with respect to the water surface.

An integration of the absorption band of the C10(PEB)-CN in chloroform yields an oscillator strength of $f = 1.00$ according to the equation[74]

$$f = \frac{4\epsilon_0 2.303 m_e c_0}{N_A e^2}\cdot\int_{\text{band}} \epsilon \, d\upsilon = 1.44 \times 10^{-19}\cdot\int_{\text{band}} \epsilon \, d\upsilon \tag{4}$$

where ϵ_0 is the permittivity of vacuum, m_e the electron mass, e the electron charge, c_0 the light speed in vacuum, N_A Avogadro's constant, ϵ the molar absortivity, and υ the frequency. The factor 1.44×10^{-19} is expressed in mol L^{-1} cm s.

The comparison of the oscillator strength obtained in solution with the apparent oscillator strength, f_{app}, calculated

(74) Kuhn, H.; Försterling, H. D. *Principles of Physical Chemistry*; John Wiley & Sons: New York, 1999.

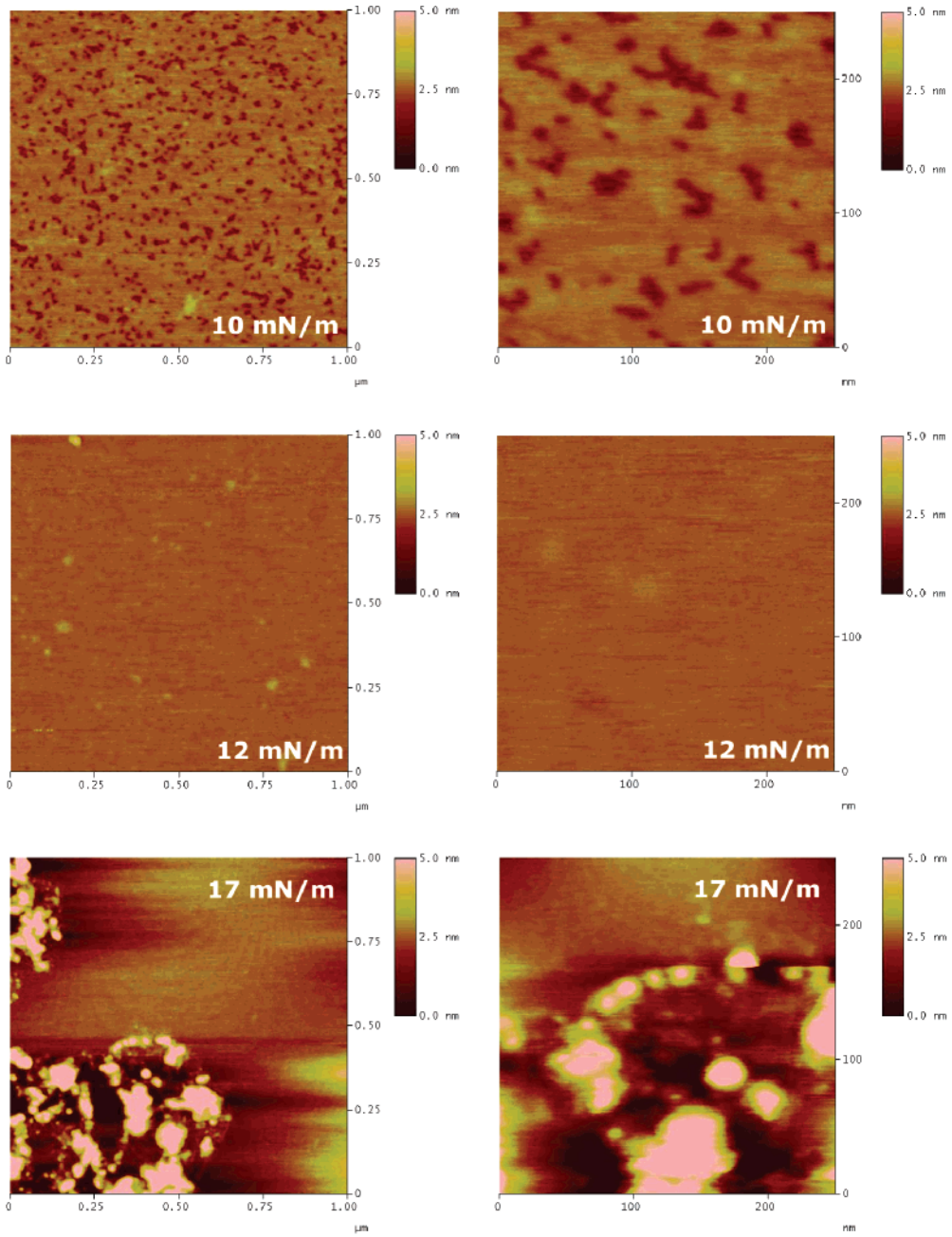

Figure 9. AFM images of a one-layer LB films of C10(PEB)CN transferred at the indicated surface pressures.

from the measured reflection spectra, allows the determination of the orientation factor using the expression

$$f_{\text{orient}} = \frac{f_{\text{app}}}{f} \tag{5}$$

where f_{app} is given by[69]

$$f_{\text{app}} = 2.6 \times 10^{-12} \cdot \int_{\text{band}} \Delta R_{\text{n}}\, \mathrm{d}\upsilon \tag{6}$$

The numeric factor 2.6×10^{-12} is expressed in nm^{-2} s. Substitution of the values obtained in eq 4 (oscillator strength) and eq 6 (apparent oscillator strength) in eq 5 give the orientation factor, which when substituted in eq 3 yields the angle, θ, formed by the normal to the surface and the dipole transition moment of the C10(PEB)CN molecule.

Figure 7 shows the $\pi-A$ isotherm (left) together with the tilt angle, ϕ (right), defined as the tilt angle with respect to the water surface ($\phi = 90 - \theta$) expressed in degrees (see Scheme 1), vs the area per molecule. From the data summarized in this figure, it can be concluded that C10-(PEB)CN molecules undergo a transition from an orientation in which they adopt an average tilt angle of ca. 35° to a more vertical position with a tilt angle close to 60° just before the overshoot. After the overshoot, there is a drastic increase in the reflection intensity (e.g., Figure 6a, reflection spectra recorded at 0.16 nm^2), which is consistent with a multilayer formation. After collapse of the monolayer, the effective path length of the surface sample increases, leading to an increase in the reflection spectrum and, in addition, the more randomly oriented molecules in the 3D aggregates that form the collapsed multilayered structure would also contribute to an increase in the ΔR values. Tilt angles beyond the overshoot have not been determined, as area per molecule values are no longer consistent with a monolayer.

The Langmuir films were transferred onto solid supports of either quartz or mica to fabricate one-layer-thick LB films. The substrates were hydrophilic and initially immersed into the subphase. The deposition ratio was close to 1 for all the substrates used.

The frequency change (Δf) for a QCM quartz resonator before and after the deposition process was determined. Taking into account the Sauerbrey equation[75]

$$\Delta f = -\frac{2f_0^{\,2}\Delta m}{A\rho_q^{\,1/2}\mu_q^{\,1/2}} \qquad (7)$$

where f_0 is the fundamental resonance frequency of 5 Hz, Δm(g) is the mass change, A is the electrode area, ρ_q is the density of the quartz (2.65 g cm^{-3}), and μ_q is the shear module (2.95×10^{11} dyn/cm^2); the C10(PEB)CN molecular weight is 359.22 g mol^{-1}, the surface coverage (Γ) is 3.4 and 3.6×10^{-10} mol cm^{-2} for films transferred at 10 and 12 mN/m, respectively, which is in excellent agreement with the estimated values for the saturated surface coverage, 3.4 and 3.6×10^{-10} mol cm^{-2}, determined from the molecular area (0.48 and 0.46 nm^2/molecule) of C10(PEB)CN at the air−water interface at the two surface pressures.

The UV−vis spectrum of a monolayer LB film of C10-(PEB)CN is similar in profile to the reflection spectrum obtained at the air−water interface for a Langmuir film at the same surface pressure, with a maximum absorption feature at 286 nm (Figure 8 shows for instance the spectrum of a 10 mN/m transferred monolayer LB film). The similarity of the spectra from the Langmuir and Langmuir−Blodgett films indicates that the H-aggregates formed at the air−water interface are transferred undisturbed onto the quartz substrate.

Atomic force microscopy is a convenient tool with which to image the film surface morphology with high spatial resolution. Representative images of films transferred to mica substrates at 10, 12, and 17 mN/m are shown in Figure 9. The films transferred from the lower surface pressure Langmuir films are very homogeneous, without obvious 3D defects. In films transferred at 10 mN/m, holes indicative of a not wholly covered surface can be seen. These holes are not apparent in the film transferred at 12 mN/m, where the mica surface is completely covered by the surface. The rms roughness is low, in the 0.3 and 0.03 nm range for films transferred at 10 and 12 mN/m, respectively. The film thicknesses were determined by scratching the films with the AFM tip, yielding values around 2.0 nm in both cases (10 and 12 mN/m). When the height of C10(PEB)CN in a vertical position (2.4 nm) is taken into account, this film thickness corresponds to a tilt angle of the molecules of 56°, in good agreement with the values obtained from reflection spectroscopy at the air−water interface. However, 3D microcrystals of irregular thickness can be seen in films transferred at surface pressures higher than the overshoot (Figure 9, transference surface pressure of 17 mN/m).

(75) Sauerbrey, G. *Z. Phys.* **1959**, *155*, 206ff.

Conclusions

Well-defined, homogeneous Langmuir films of the tolan derivative C10(PEB)CN can be fabricated at the air−water interface on a pure water subphase. Two-dimensional H-aggregates are formed as soon as the organic compound is spread onto the water surface and apparently represent a minimum free energy conformation for the system. A significant degree of order is progressively achieved upon the compression process, accompanied by a gradual tilt of the molecules from an initial angle of 35° between the long axis of the molecule and the water surface, to a value of nearly 60° before the collapse of the monolayer into an undefined, multilayer structure. The Langmuir films are transferable onto solid supports by the vertical dipping method with a deposition ratio of 1. Furthermore, UV−vis and AFM studies have demonstrated that the Langmuir film is transferred onto the substrates keeping the same H-aggregation and orientation than the floating monolayers.

Acknowledgment. The authors are grateful for financial assistance from MEC (Spain) and fondos FEDER in the framework of Projects BQU2003-01765 and CTQ2006-05236 as well as for supporting A.V. through the award of an FPU studentship. We also thank ONE NorthEast for financial support through the Durham UIC Nanotechnology (P.J.L.).

CM062524P